Pharmacogn. Res., 2026; 18(2):460-475.
https://www.phcogres.com

Original Article

Aquilaria agallocha Mitigates MPTP Induced Parkinson's Disease by Targeting the BDNF/GDNF and NRF2 Pathways: A Network Pharmacology and an *in vivo* Study

Preetu Shukla[1,2], Nilay Solanki[1,*], Prarambh SR Dwivedi[3]

[1]Department of Pharmacology, Ramanbhai Patel College of Pharmacy, Charotar University of Science and Technology, CHARUSAT Campus, Changa, Gujarat, INDIA.
[2]Department of Pharmacology, Motherhood University Roorkee, Haridwar, Uttarakhand, INDIA.
[3]Department of Pharmacology, NGSM Institute of Pharmaceutical Sciences (NGSMIPS), NITTE (Deemed to be University), Mangalore, Karnataka, INDIA.

ABSTRACT

Background: Parkinson's Disease (PD) is a progressive neurodegenerative disorder marked by the neuronal death and a complex, multifaceted etiology. The present study aimed to investigate the potential of *Aquilaria agallocha* (AA; Family: Thymelaceae) leaf extract on MPTP-induced Parkinson's disease in Wistar rats, utilising *in silico* and *in vivo* protocols. **Materials and Methods:** Bioactive-target interactions were studied via network pharmacology and docking. Protein-ligand binding was assessed using AutoDock Vina. Parkinson's disease was induced in male Wistar rats via intranasal MPTP. Rats were treated with extract doses (50, 100, 200 mg/kg) and levodopa. Behavioural tests (open field, rotarod, beam walk, grid hanging), neurochemical assays (TBARS, SOD, catalase, dopamine), and ELISA-based biomarker estimation (GDNF, BDNF, LRRK2, NRF2) were conducted. **Results:** Network pharmacology revealed 45 Parkinson's-related targets and key pathways, including apoptosis, PI3K-Akt, and neurotrophin signalling. Molecular docking showed strong binding of 12-deoxyphorbol and Clemiscosin D with MAPK3/MAPK1, BDNF/GDNF, LRRK2, and NRF2. In an *in vivo*, AA extract significantly improved motor performance in rotarod, open field, and grid hanging tests. Biochemical assays showed reduced MDA and restored catalase and antioxidant levels. Dopamine, BDNF, GDNF, and LRRK2 levels increased significantly with treatment, confirming neuroprotective effects. AA-200 mg/kg dose was most effective, often comparable to levodopa, supporting its potential in Parkinson's disease therapy. **Conclusion:** *A. agallocha* is rich in bioactive compounds, including Clemiscosin D, 12-deoxyphorbol-13, a phorbol, which are known for their potent antioxidant and anti-inflammatory properties, and exerts neuroprotective effects by modulating key molecular targets involved in oxidative stress.

Keywords: Parkinson's Disease, MPTP, *Aquilaria agallocha*, Network Pharmacology, BDNF, GDNF.

Correspondence:
Dr. Nilay Solanki
Associate Professor, Department of Pharmacology, Ramanbhai Patel College of Pharmacy, Charotar University of Science and Technology, CHARUSAT Campus, Changa-388421, Gujarat, INDIA.
Email: nivyrx@gmail.com; nilaysolanki.ph@charusat.ac.in

Received: 14-08-2025;
Revised: 27-10-2025;
Accepted: 08-12-2025.

INTRODUCTION

Parkinson's Disease (PD) is a progressive neurodegenerative disorder that predominantly impairs motor function. It is characterized by the selective degeneration of dopaminergic neurons in the substantia nigra pars compacta, a region critical for the regulation of voluntary movement. The resulting dopaminergic deficit in the striatum leads to the hallmark motor symptoms of the disease, including resting tremors, muscle rigidity, bradykinesia (slowness of movement), and postural instability (Figure 1) (Girish *et al.*, 2015; Giri *et al.*, 2020). As the disease progresses, patients often develop a range of non-motor symptoms such as cognitive impairment, mood disturbances, sleep disorders, and autonomic dysfunction, all of which contribute to a significant decline in quality of life (Bagewadi *et al.*, 2018; Chen *et al.*, 2018). It is estimated that 6.3 million people suffer from PD worldwide (Corona *et al.*, 2018). The incidence has ranged from 4.5 to 21 cases per 100,000 population per year. Genetic mutations in critical neurotrophic and regulatory genes such as LRRK2, GDNF, and NRF2 contribute to autophagy-lysosomal system dysfunction and impaired protein clearance, resulting in the accumulation of misfolded α-synuclein aggregates (Dash *et al.*, 2008; Delenclos *et al.*, 2019). These aggregates promote apoptosome formation and apoptosis, aggravating neuronal loss. Simultaneously, oxidative stress, a central pathogenic factor, is exacerbated by both intrinsic mutations and extrinsic factors such as environmental toxins, leading to elevated Reactive Oxygen Species (ROS) levels. The ROS burden activates microglia and astrocytes, triggering NF-κB signalling and the release of

DOI: 10.5530/pres.20260160

pro-inflammatory cytokines and chemokines, which contribute to neuroinflammation. Moreover, ROS and excessive calcium influx through NMDA receptor-mediated excitotoxic pathways further amplify neuronal injury.

Available therapeutic approaches, including dopaminergic agents (e.g., levodopa), physical rehabilitation, and surgical interventions such as deep brain stimulation, primarily aim to alleviate symptoms rather than halt disease progression (Gopi *et al*., 2019; Gopinath *et al*., 2015). The global prevalence of PD is projected to increase with rising life expectancy, underscoring the urgent need for novel therapeutic agents that can modify disease progression and improve patient outcomes (Oraon *et al*., 2019). The exploration of phytochemicals and traditional medicinal plants has garnered significant interest. *Aquilaria agallocha*, commonly known as Agarwood, has a long history of use in traditional systems of medicine such as Ayurveda, Traditional Chinese Medicine (TCM), and Unani, particularly for the treatment of neurological disorders, inflammation, and oxidative stress-related conditions (Hashim *et al*., 2016; Kumaree *et al*., 2025). This plant extract appears to mitigate ROS levels, inhibit α-synuclein aggregation, downregulate pro-apoptotic signalling, and suppress neuroinflammation. These actions collectively protect against dopaminergic neuron loss and thus attenuate neurodegeneration associated with PD. Recent experimental studies suggest that these constituents may offer neuroprotective effects, potentially through the mitigation of oxidative stress and inflammatory pathways involved in the pathophysiology of neurodegenerative diseases such as PD (Leao *et al*., 2017). Hence, this study aims to assess the potential of *Aquilaria agallocha* and identify potential targets modulated by it against Parkinson's disease.

MATERIALS AND METHODS

Chemicals, reagents, and biological kits

All the chemicals and reagents were used in analytical grade and purchased from Himedia-India, and ELISA kits from ELK Biotechnology Co., Ltd.

Plant authentication and extraction process

Fresh leaves of *Aquilaria agallocha* were obtained from a commercial source in Anand, Gujarat & were authenticated by Dr. Komal Patel from Parul Institute of Ayurved, Vadodara, with Specimen voucher (PU/PIA/DG-cert-100(b)23/12/2021). The leaves were dried in sunlight, converted into dried powder form and stored in an air-tight container. Standardised powdered plant materials extracted with 50% ethanol in water, using the Soxhlet extraction technique to reduce solvent use and maximise extraction efficiency. The hydro-alcoholic extract of the plant was collected, lyophilized, and stored (Lee *et al*., 2021).

Experimental animals, treatment groups and induction of Parkinsons disease

The animals (Male Albino Wistar rats) were purchased from CCSEA registered facility, Ahmedabad, Gujarat, India (Protocol no. - PIPR985/2023/01/02) with a weight range of 150-200 grams. A total of 36 male rats were randomly divided into the different groups (n = 6 per group), with treatments administered according to the study design: Normal Control (NC) received saline and disease control (MPTP) received MPTP (0.1 mg per rat) via intranasal route. Other groups consisted of treatment with different doses of *A. agallocha* extract (AA) (50, 100, and 200 mg/kg via oral route) and standard levodopa (30 mg/kg via *i.p.*) after induction with MPTP, named as AA-50, AA-100, AA-200, and LD, respectively. MPTP-HCl was dissolved in sterile saline (0.9% NaCl), final concentration: 0.1 mg MPTP per nostril per day, with adjusted pH up to 7.4, and filter-sterilised (0.22 µm filter). Lightly anesthetize the rat (with ketamine/xylazine). Rats were placed in a supine position (on its back) at a slight incline. Use a micropipette to apply 10 µL of MPTP solution into each nostril (Miniyar *et al*., 2008).

Network Pharmacology

Identification of bioactives and targets from Aquilaria agallocha with respect to Parkinson's disease

The pytoconstituents from the plants *A. agallocha* (leaf) were retrieved from Chemical Entities of Biological Interest (ChEBI; https://www.ebi.ac.uk/chebi/) and Indian Medicinal Plants, Phytochemistry and Therapeutics 2.0 (IMPPAT 2.0; https://cb.imsc.res.in/imppat/) database. The targets modulated by the bioactives were sourced from the DIGEP-Pred 2.0 database (https://www.way2drug.com/digep-pred/), keeping pharmacological activity greater than 0.9. The targets involved in the pathogenesis of Parkinson's disease were retrieved from the Comparative Toxicogenomics Database (CTD; https://ctdbase.org/). The targets possessing an inference score greater than 70 were included for matching (Duyu *et al*., 2020; Lakshmi *et al*., 2023).

Network construction and Gene ontology analysis

The targets identified to be modulated via the bioactives were matched with targets involved in the pathogenesis of Parkinson's disease. The matched targets were further subjected to STRING (https://string-db.org/) to obtain the protein-protein interaction network. The KEGG pathway and gene ontology enrichment analysis were performed using STRING, and potential pathways involved in the pathogenesis of Parkinson's disease were identified. Further, a network was constructed using Cytoscape representing the plant-bioactive-pathway-protein interaction network. This network was analyzed as a directed graph, where node size and color were mapped according to edge count. Advanced network topology analysis was conducted, focusing on parameters such

as node degree distribution and betweenness centrality, along with eccentricity, neighbourhood connectivity, in-degree and out-degree distributions to assess network robustness and target relevance (Sahu *et al.*, 2025; Subramanian *et al.*, 2024).

Molecular docking

Preparation of Proteins

The structure of proteins were inquired in UniProt (*https://www.uniprot.org/*) database to identify available targets in Protein Data Bank (RCSB; *https://www.rcsb.org/*). The targets not available in PDB were modelled using the known FASTA sequence *via* SWISS-MODEL (*https://swissmodel.expasy.org*). The protein was prepared by removing hetero-atoms and was saved in .pdb format using the Discovery studio visualizer. The energy was minimised for all the proteins using the MMFF94 force field (Rahman *et al.*, 2012).

Preparation of Ligand

The 3D conformation of ligands was retrieved from the PubChem database in .sdf format. The 3d conformer was converted into .pdb using Discovery Studio Visualizer 2019 (BO*VIA* Discovery Studio Visualizer; *https://discover.3ds.com/discovery-studio-visualizer-download)*. The energy of the ligand was minimized and converted into .pdbqt format before subjecting it to docking (Rao *et al.*, 2020).

Protein-ligand docking

The docking was performed using Auto Dock Vina, and the binding energy was assessed with proteins involved in the pathogenesis of Parkinson's disease. The parameters like binding energy, number of hydrogen bonds, number of hydrogen bond residues, number of π-π interactions, along with their residues, were utilised for analysing the binding affinity of ligands. The top three complexes, which possessed the highest binding affinity, were visualized (Ravi *et al.*, 2018).

Neurobehavioral assessments

Open Field Test

The Open Field Test was performed using an apparatus measuring 100 × 100 × 40 cm, with the floor lined with resin-coated cloth and divided into 25 equal squares. Each rat was individually placed in one corner of the field and allowed to explore freely for 300 seconds. During this period, behavioural parameters such as peripheral and central locomotion, rearing, and grooming activities were observed and recorded. The apparatus was cleaned with 70% ethanol between trials to eliminate residual olfactory cues. All assessments were conducted in a quiet, dimly lit environment, and animals were acclimatized prior to testing (Sikdar *et al.*, 2017).

Narrow Beam Walk Test

The Narrow Beam Walk Test was employed to assess motor coordination and balance. A narrow wooden beam measuring 100 cm in length and 1 cm in width was elevated 100 cm above the ground. Each trained rat was gently placed at one end of the beam and allowed to traverse to the opposite end. During the trial, the time taken to cross the beam and the number of foot-slip errors were recorded. The beam was cleaned with 70% ethanol between trials to remove any scent trails. Tests were conducted in a quiet environment to minimise external distractions (Tanaka *et al.*, 2013).

Rotarod Test

The rotarod test was used to evaluate motor coordination, balance, and motor learning in rats. The apparatus consisted of a rotating rod with gradually increasing speeds ranging from 5 to 40 revolutions per minute (rpm). Each rat was placed individually on the rod, and the latency to fall-the time the animal remained on the rotating rod-was recorded. Prior to the actual test, animals were given training sessions to familiarize them with the apparatus. The rod was cleaned with 70% ethanol between trials to eliminate olfactory cues. All tests were conducted in a quiet environment to reduce stress (Tang, Y., & Le, W., 2016).

Grid Hanging Test

Neuromuscular strength was assessed using the grip hanging test based on the method described by Pérez and Palmiter. Each rat was gently lifted by the tail and placed at the center of a horizontal wire grid. Once the animal firmly grasped the grid using both forelimbs and hindlimbs, the grid was carefully inverted to a suspended position approximately 40 cm above a cushioned surface. The latency to fall, defined as the time the animal was able to hang onto the inverted grid, was recorded with a maximum cutoff time of 60 sec. The grid was cleaned with 70% ethanol between trials to eliminate scent cues. All tests were conducted in a quiet environment to minimize stress (Wang *et al.*, 2018).

Neurochemical estimations

Lipid Peroxidation Assay

Lipid peroxidation in brain tissues was quantified by estimating Thiobarbituric Acid Reactive Substances (TBARS). A volume of 0.2 mL of tissue homogenate was mixed with 0.4 mL of 5% Trichloroacetic Acid (TCA) and 0.4 mL of 0.67% Thiobarbituric Acid (TBA) in an Eppendorf tube. The reaction mixture was centrifuged at 3,500 rpm for 15 min. The resulting supernatant was then transferred into a fresh tube and heated in a boiling water bath for 10 min to complete the reaction. After cooling to room temperature, the absorbance was measured at 535 nm using a spectrophotometer (Xie *et al.*, 2021).

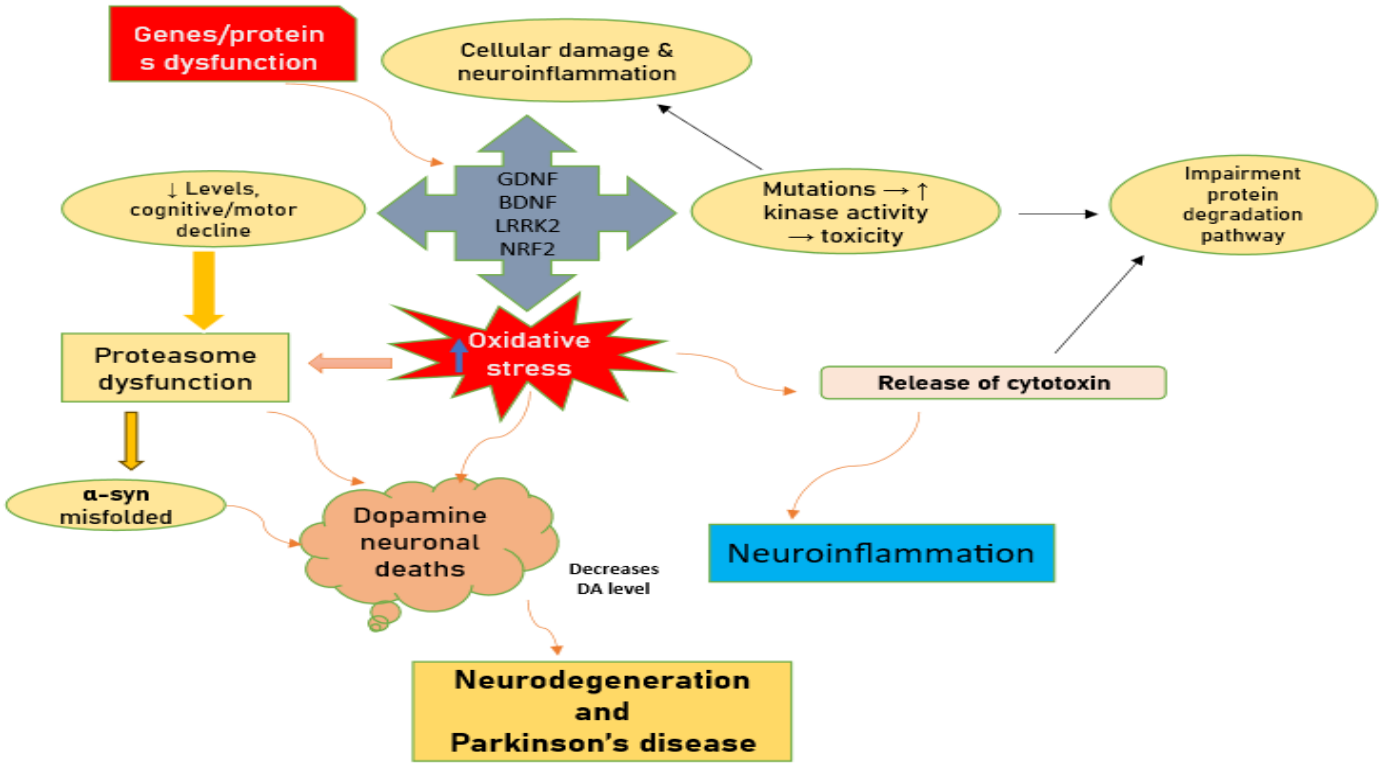

Figure 1: Pathophysiology of Parkinson's disease.

Superoxide Dismutase Activity

Superoxide Dismutase (SOD) activity was assessed by measuring the inhibition of Nitro Blue Tetrazolium (NBT) reduction. The assay mixture consisted of 0.1 mL of Post-Mitochondrial Supernatant (PMS), 50 mM phosphate buffer (pH 7.4), 1.0 mM xanthine, and 57 µM NBT. The reaction was initiated by the addition of 50 mU of xanthine oxidase and incubated at room temperature for 15 minutes. The reduction of NBT to formazan, indicating superoxide generation, was monitored spectrophotometrically by measuring the absorbance at 550 nm. A decrease in absorbance corresponds to increased SOD activity, reflecting its ability to scavenge superoxide radicals (Zheng *et al.*, 2019).

Catalase Activity

Catalase activity was determined based on the decomposition of Hydrogen Peroxide (H_2O_2). The reaction mixture consisted of 0.019 M H_2O_2, 50 mM phosphate buffer (pH 7.0), and 0.05 mL of PMS, with a total reaction volume of 3.0 mL. The decrease in absorbance due to the breakdown of H_2O_2 was recorded at 240 nm. Enzymatic activity was expressed as the amount of H_2O_2 decomposed per minute per milligram of protein (nmol H_2O_2/min/mg protein) (Abolarin *et al.*, 2024).

Dopamine Assay

Striatal dopamine levels were quantified using High-Performance Liquid Chromatography (HPLC) coupled with Electrochemical Detection (ECD). Tissue samples were homogenized and sonicated in ice-cold 0.1 M perchloric acid containing 0.01% EDTA, followed by centrifugation. A 10 µL aliquot of the supernatant was injected into the HPLC system equipped with a Beckman Gold 118 integrator. The mobile phase consisted of 3% methanol, 7% acetonitrile, and 90% aqueous buffer. The flow rate was maintained at 0.3 mL/min. Dopamine concentrations were calculated based on peak areas and expressed as ng per mg of brain tissue (Abushouk *et al.*, 2017).

Estimation of GDNF, BDNF, LRRK2, and NRF2 as biomarker of Parkinson's disease

GDNF, BDNF, LRRK2 and NRF2 biomarkers were assessed by rat Elisa kit (Catalog No. ELK-20,431/1424/SG-10643/7238) purchased from ELK Biotechnology Co., Ltd. The absorbance was read against blank at 450 nm with a microtiter plate reader. The Optical Density (OD) values were obtained to plot a standard curve, used to determine concentration of particular biomarkers in the samples (Duyu *et al.*, 2020).

Histopathology

Histopathological evaluation of the striatum was performed to assess neuronal integrity and glial response across experimental groups. After the completion of behavioural and biochemical assessments, rats were euthanised, and brain tissues were carefully dissected and fixed in 10% neutral buffered formalin for 24-48 hr. The tissues were then processed through graded alcohols, cleared in xylene, and embedded in paraffin wax. Coronal sections of

5 µm thickness were cut using a microtome and stained with Hematoxylin and Eosin (H&E). Stained sections were examined under a light microscope at 40× magnification for morphological changes, including neuronal degeneration, gliosis, necrosis, and the presence of Lewy body-like inclusions.

Statistical analysis

All data were expressed as Mean±Standard Deviation (SD). Comparisons between the means of different groups of animals and those of control animals were performed using one-way Analysis of Variance (ANOVA). Significance was set at $p<0.05$. When the data were statistically significant, the ANOVA test was followed by Tukey's HSD test.

RESULTS

Network analysis

A Protein-Protein Interaction (PPI) network with 45 nodes and 700 edges showed high connectivity (average node degree 31.1) and strong clustering (coefficient 0.837), indicating tightly linked functional groups. The network was statistically significant (p<1.0e-16), suggesting non-random, biologically relevant interactions. KEGG pathway analysis identified key pathways involved in Parkinson's disease, including apoptosis, TNF signalling, PI3K-Akt, HIF-1, mitophagy, and neurotrophin signalling, highlighting roles in inflammation, cell survival, and mitochondrial function. Some overlap with Alzheimer's and ALS pathways suggests common neurodegenerative mechanisms. The compound 12-deoxyphorbol-13-(3E,5E-decadienoate) showed a strong central role, while proteins like MAPK3, TP53, RELA, and NFKB1 emerged as key regulators, supporting their importance in PD-related signalling (Table 1, Figures 2 and 3).

Molecular docking

Docking results showed that both 12-deoxyphorbol-13-(3E,5E-decadienoate) and Clemiscosin D exhibit strong binding affinities with MAPK3 and MAPK1, with binding energies of -9.1 and -8.6 kcal/mol, respectively. 12-deoxyphorbol formed stable interactions with MAPK3 through hydrogen bonds (e.g., SER170, ASN171) and hydrophobic contacts (e.g., LEU124). Clemiscosin D showed favourable binding with MAPK1 via multiple hydrogen bonds (e.g., GLN103, ASP165) and hydrophobic residues (e.g., VAL37), with a slightly better binding energy (-9.0 kcal/mol). Clemiscosin D also interacted strongly with Dopamine-related targets, showing a binding energy of -8.9 kcal/mol and key interactions with residues like ASN70 and PRO139. Overall, Clemiscosin D demonstrated higher binding stability and broader therapeutic potential, especially via MAPK3/MAPK1 signalling pathways (Figure 4, Table 1).

Gene Ontology (GO) Enrichment Analysis

GO enrichment analysis using the STRING database revealed significant enrichment across Cellular Component (CC), Molecular Function (MF), and Biological Process (BP) categories. In CC, the *endomembrane system* (GO:0012505) was most significantly enriched (FDR = 0.00032), involving 27 genes. In MF, *protein binding* (GO:0005515) showed the highest significance (FDR = 1.17E-14) with 44 associated genes. For BP, *response to oxygen-containing compound* (GO:1901700) was the most enriched term (FDR = 6.40E-31), involving 38 genes. These results indicate strong involvement of the selected targets in cellular localisation, binding functions, and oxidative stress-related biological processes relevant to Parkinson's disease (Figure 5).

NEUROBEHAVIORAL ESTIMATIONS

Effect of *A. agallocha* on Rota Rod test

The Normal Control (NC) group exhibited the highest performance, with a mean retention time of 92.33 ± 4.71 sec, indicating intact motor function. In contrast, the MPTP group showed a significant reduction in performance, with a mean time of 55.5 ± 3.39 sec (#p < 0.05), confirming MPTP-induced motor impairment. Treatment with *A. agallocha* at 50 mg/kg (AA-50) yielded a non-significant improvement (58.33 ± 9.86 sec; ns), while AA-100 (64.5 ± 9.05 sec) and AA-200 (79.5 ± 15.39 seconds)

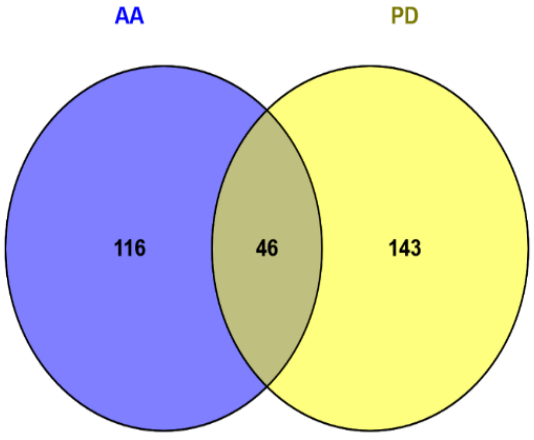

Figure 2: A Venn diagram representation of the targets modulated by *Aquilaria agallocha* against Parkinson's disease.

showed a dose-dependent, statistically significant recovery in retention time compared to the MPTP group (***$p < 0.0001$). Levodopa (LD) treatment resulted in a substantial restoration of motor coordination (87.17 ± 6.43 sec), closely approximating the NC group. These results confirm that *A. agallocha*, particularly at 100 and 200 mg/kg, significantly mitigates MPTP-induced motor deficits (Figure 6).

Effect of *A. agallocha* on open field test

The Normal Control (NC) group showed high locomotor activity, with a mean exploration time of 111.17 ± 8.33 seconds. MPTP administration significantly reduced this activity, with animals showing a mean time of only 40.5 ± 11.79 sec (#$p < 0.05$), indicating dopaminergic damage and reduced spontaneous movement. Treatment with *A. agallocha* at 50 mg/kg (AA-50) moderately improved performance (63.17 ± 15.38 seconds; *$p < 0.01$), while AA-100 (65.00 ± 18.84 sec) and AA-200 (80.83 ± 11.39 sec) showed significant dose-dependent recovery (**$p < 0.001$ to *$p < 0.0001$). Levodopa (LD) was similarly effective, yielding a mean time of 88.83 ± 6.46 seconds, reflecting substantial restoration of locomotor function (Figure 6).

Effect of *A. agallocha* on Grid hanging test

The Normal Control (NC) group demonstrated robust performance with a mean hanging time of 92.33 ± 6.45 seconds, indicating intact neuromuscular endurance. In contrast, the MPTP group exhibited a significant reduction in hanging ability, with a mean time of 41.83 ± 2.79 seconds (#$p < 0.05$), reflecting muscle weakness associated with dopaminergic degeneration. Treatment with *A. agallocha* at 50 mg/kg (AA-50) produced a marginal increase (45.67 ± 3.39 sec; ns), which was not statistically significant. However, AA-100 (60.33 ± 4.85 sec) and AA-200 (83.17 ± 4.99 sec) significantly enhanced neuromuscular strength compared to the MPTP group (***$p < 0.0001$), suggesting a dose-dependent effect. Levodopa (LD) treatment led to a mean time of 92.17 ± 4.97 sec, nearly restoring function to normal levels (Figure 6).

Effect of *A. agallocha* on Narrow beam test

The Normal Control (NC) group displayed optimal performance, crossing the beam in 10.67 ± 0.82 seconds. In contrast, MPTP-treated mice showed a significant delay in crossing, with a mean time of 17.83 ± 1.47 seconds (#$p < 0.05$), indicating impaired motor coordination. Treatment with *A. agallocha* at 50 mg/kg (AA-50) resulted in a non-significant improvement (16.67 ± 1.21 sec; ns). However, AA-100 (13.00 ± 2.61 sec) and AA-200 (14.33 ± 1.21 sec) demonstrated significant reductions in crossing time compared to the MPTP group (**$p < 0.001$ and ***$p < 0.0001$, respectively), indicating enhanced balance and coordination. The Levodopa (LD) group exhibited substantial improvement, with a mean crossing time of 12.50 ± 1.05 sec, closely approaching that of the NC group (Figure 6).

NEUROCHEMICAL ESTIMATIONS

Effect of *A. agallocha* on Lipid peroxidase

the MPTP-treated group exhibited a significant increase in MDA levels (6.96 ± 0.75 nmol/mg protein) compared to the normal control group (2.94 ± 0.78 nmol/mg protein, #$p < 0.05$), indicating

Table 1: The binding energies of bioactives with hub targets.

Target	Bioactive (Binding energy (kcal/mol))			
	A	B	C	D
TP53	-7.6	-6.7	-4.9	-5.4
MAPK3	-9.1	-9.1	-6.2	-5.8
MAPK1	-8.6	-9	-5.6	-6.3
GSH	-7.1	-7.7	-5.6	-6.8
D2	-6.4	-8.9	-5	-6.2
BDNF	-7.2	-6.3	-4.2	-4.8
GDNF	-7.6	-6.9	-4.7	-5.6
NRF2	-6.4	-6.9	-5.3	-5.1
LRRK2	-6.9	-6.1	-5.2	-5.4
Pink1	-6.9	-7.6	-5.5	-6.4
Parkin	-7.2	-7.5	-5.8	-6.6

Where A: 12-deoxyphorbol-13-(3E,5E-decadienoate); B: Clemiscosin D; C: Ethyl benzoate; D: Levodopa (standard).

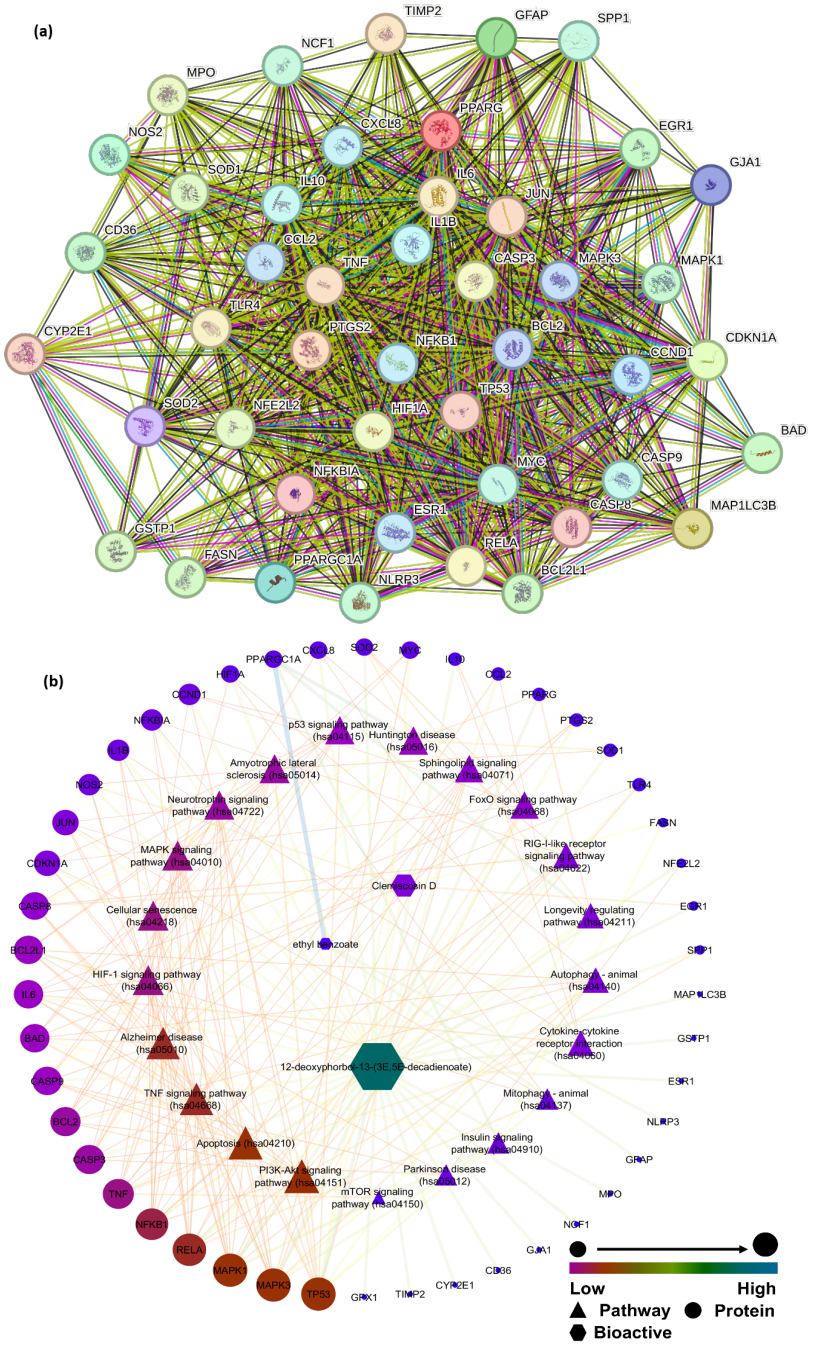

Name	ASPL	BC	CC	Degree	NC	NDE	TC
12-deoxyphorbol-13-(3E,5E-decadienoate)	1.59	0.51	0.63	40	5.03	40	0.18
Clemiscosin D	2.67	0.02	0.38	6	6.33	6	0.28
ethyl benzoate	4.06	0.06	0.25	3	2	3	0.33
PI3K-Akt signaling pathway (hsa04151)	2.32	0.04	0.43	15	8.53	15	0.34
Apoptosis (hsa04210)	2.35	0.03	0.43	14	9.79	14	0.40
TNF signaling pathway (hsa04668)	2.38	0.03	0.42	13	8.38	13	0.34
Alzheimer disease (hsa05010)	2.38	0.03	0.42	13	8.92	13	0.36
HIF-1 signaling pathway (hsa04066)	2.52	0.02	0.40	10	8.80	10	0.39
MAPK3	2.00	0.06	0.50	14	11.57	14	0.25
MAPK1	2.00	0.06	0.50	14	11.57	14	0.25
TP53	2.00	0.08	0.50	14	10.86	14	0.23
RELA	2.06	0.05	0.49	13	12.15	13	0.27
NFKB1	2.09	0.04	0.48	12	12.75	12	0.28

Figure 3: (a) The protein-protein interaction of targets modulated via *Aquilaria agallocha* against Parkinson's disease; (b) The bioactive-protein-pathway interaction for the targets modulated via *Aquilaria agallocha* against Parkinsonism disease; (c) The properties of network with respect to Average Shortest Path Length (ASPL), Betweenness Centrality (BC), Closeness Centrality (CC), Neighbourhood Connectivity (NC), Number of Directed Edges (NDE), and Topological Coefficient (TC).

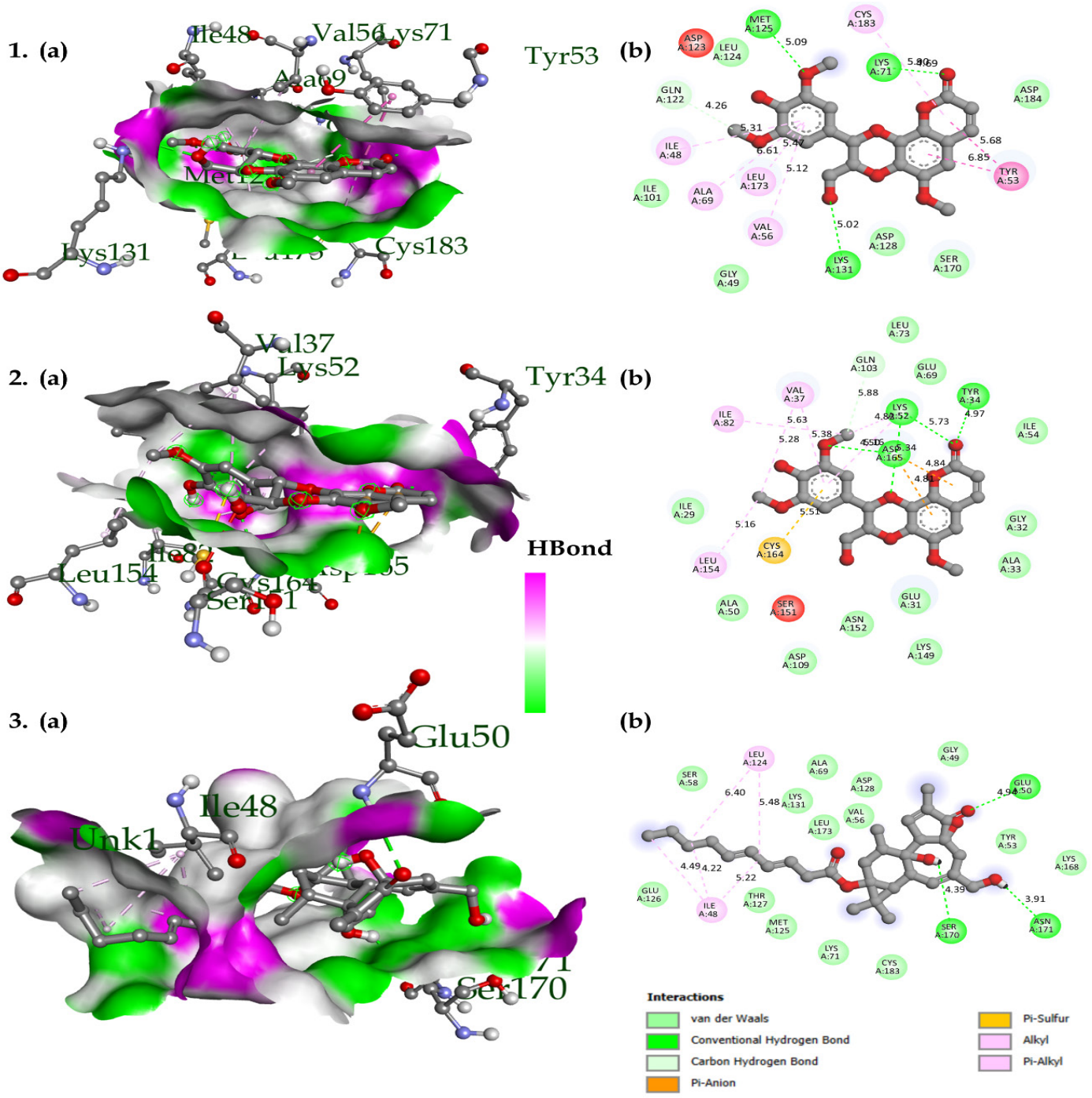

Figure 4: The top 3 complexes possessing the highest binding affinity. Where, (a) 3D and (b) 2D; 1. MAPK3-Clemiscosin D, 2. MAPK1-Clemiscosin D, and 3. MAPK3-12-deoxyphorbol-13-(3E,5E-decadienoate).

enhanced lipid peroxidation and oxidative stress. Treatment with *A. agallocha* notably decreased MDA levels in a dose-dependent manner. The AA-50 group showed a reduction to 3.44 ± 0.27 (***$p < 0.0001$ vs MPTP), AA-100 to 3.04 ± 0.86 (***$p < 0.0001$), and AA-200 to 2.56 ± 0.12 nmol/mg protein (***$p < 0.0001$), approaching normal values. The standard levodopa-treated group also showed reduced MDA levels (2.46 ± 0.10), with no significant difference when compared to the AA-200 group (ns) (Figure 7).

Effect of *A. agallocha* on Catalase activity

MPTP administration significantly reduced catalase activity (31.4 ± 1.65 U/mg protein) compared to the normal control

group (52.0 ± 0.91 U/mg protein, #$p < 0.05$), indicating oxidative impairment. Treatment with *A. agallocha* led to a dose-dependent restoration of catalase activity. The AA-50 group showed a mild improvement (34.42 ± 2.35 U/mg, *$p < 0.01$ vs MPTP), while the AA-100 group exhibited a greater recovery (40.64 ± 0.48 U/mg, *$p < 0.01$). Notably, AA-200 significantly restored catalase activity to near-normal levels (46.74 ± 0.42 U/mg, *$p < 0.01$), comparable to the levodopa-treated group (48.88 ± 0.31 U/mg, vs AA-200) (Figure 7).

Effect of *A. agallocha* on antioxidant SOD

SOD activity was significantly reduced in the MPTP group (3.14 ± 0.10 U/mg protein) compared to the normal control (5.56 ± 0.10 U/mg protein, #$p < 0.05$), indicating compromised enzymatic antioxidant defense. Treatment with *Aquilaria agallocha* restored SOD activity in a dose-dependent manner. The AA-50 group showed moderate improvement (3.78 ± 0.12 U/mg, ***$p < 0.0001$ vs MPTP), while the AA-100 group further improved activity (4.52 ± 0.08 U/mg, ***$p < 0.0001$). Notably, the AA-200 group almost normalized SOD levels (5.68 ± 0.20 U/mg), which was comparable to the levodopa-treated group (5.32 ± 0.08 U/mg, ns) (Figure 7).

Effect of *A. agallocha* on brain dopamine levels

MPTP administration resulted in a significant depletion of dopamine levels in brain tissue (4.14 ± 0.11 µg/g tissue) when compared to the normal control group (12.40 ± 0.19 µg/g, #$p < 0.05$), reflecting dopaminergic neuronal loss. Treatment with *A. agallocha* significantly restored dopamine levels in a dose-dependent fashion. The AA-50 group showed modest recovery (5.72 ± 0.13 µg/g, ***$p < 0.0001$ vs MPTP), while AA-100 and AA-200 groups demonstrated progressive restoration (7.34 ± 0.10 and 9.46 ± 0.10 µg/g, respectively, ***$p < 0.0001$). The AA-200 group nearly reached the dopamine levels observed in the levodopa-treated group (10.76 ± 0.11 µg/g, ns vs AA-200), indicating comparable efficacy (Figure 7).

Estimation of GDNF, BDNF, LRRK2, and NRF2 as biomarker of Parkinson's disease

Effect of A. agallocha on brain BDNF levels

The Normal Control (NC) group showed a consistent mean BDNF level of 0.452 ± 0.004 OD units, indicating normal neurotrophic support. MPTP administration led to a significant decline in BDNF expression (0.32 ± 0.034 OD; #$p < 0.05$), reflecting neurodegenerative insult. Treatment with *A. agallocha* at 50 mg/kg (AA-50) moderately elevated BDNF levels (0.55 ± 0.000 OD). However, AA-100 (0.702 ± 0.005 OD) and AA-200 (0.852 ± 0.005 OD) resulted in substantial, dose-dependent increases in BDNF expression (***$p < 0.0001$). Levodopa (LD) treatment also restored BDNF levels (0.756 ± 0.006 OD) comparable to the highest AA dose (Figure 8).

Effect of *A. agallocha* on brain GDNF levels

The MPTP group showed a marked decline in GDNF expression (0.25 ± 0.02 OD), significantly lower than the normal control group (1.09 ± 0.03 OD, #$p < 0.05$). Treatment with *A. agallocha* led to a dose-dependent restoration of GDNF levels. The AA-50 group showed a partial but significant improvement (0.65 ± 0.01 OD, ***$p < 0.0001$ vs MPTP), while AA-100 and AA-200 groups exhibited near-complete recovery (0.95 ± 0.01 and 1.11 ± 0.02 OD, respectively; ***$p < 0.0001$ vs MPTP). A significant difference was observed between the AA-200 and LD groups, indicating that *A. agallocha* at 200 mg/kg was as effective as the standard levodopa treatment in restoring GDNF levels (Figure 8).

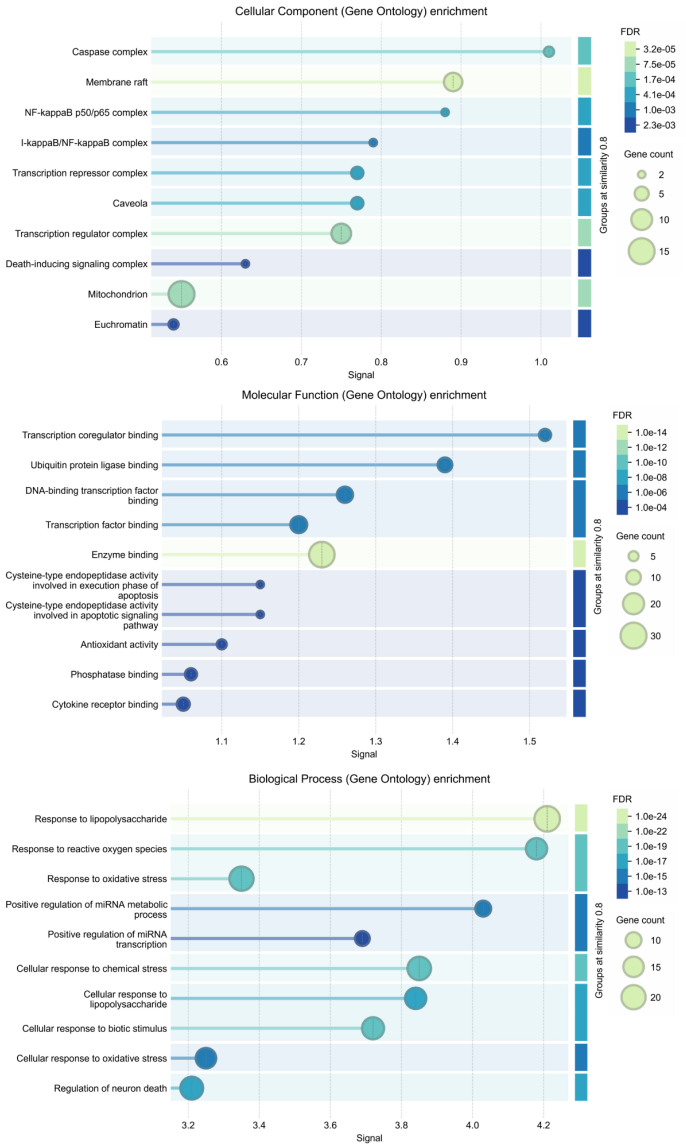

Figure 5: The enriched gene ontology for the top 10 cellular components, molecular functions, and biological processes modulated via *Aquilaria agallocha* against Parkinsonism disease.

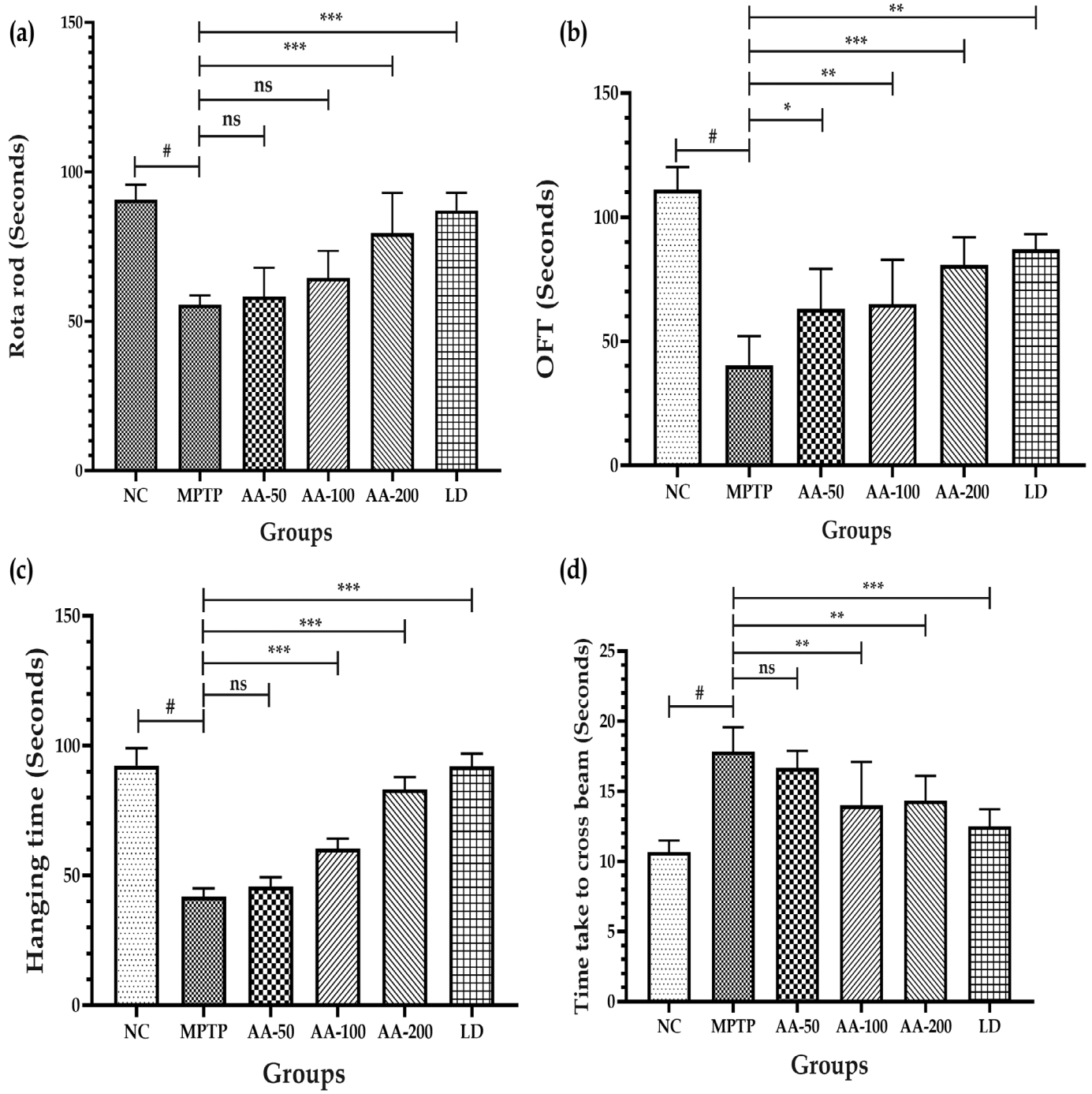

Figure 6: Neurobehavioral estimations on treatment with *Aquilaria agallocha* assessed via (a) Rotarod test, (b) open field test, (c) grid hanging test, and (d) narrow beam test. Data are expressed as mean ± SD (n=6) and analysed using one-way ANOVA followed by Tukey's multiple comparison test. $^{\#}p<0.05$ as compared to NC, $^{*}p < 0.01$, $^{**}p < 0.001$, $^{***}p < 0.0001$ vs MPTP group, and ns: non-significant.

Effect of *A. agallocha* on brain NRF2 levels

MPTP administration significantly elevated NRF2 expression (0.94 ± 0.02 OD) compared to the normal control group (0.40 ± 0.01 OD, $\#p < 0.05$), indicating a possible compensatory oxidative stress response. Treatment with *A. agallocha* resulted in a dose-dependent reduction in NRF2 levels. The AA-50 group showed a moderate but significant decrease (0.74 ± 0.01 OD, $^{*}p < 0.05$ vs MPTP), while AA-100 and AA-200 groups further reduced NRF2 expression (0.62 ± 0.01 and 0.47 ± 0.01 OD, respectively; $^{**}p < 0.01$ and $^{***}p < 0.001$ vs MPTP). The AA-200 group closely approached the NRF2 levels of the normal control, suggesting attenuation of oxidative stress. The standard levodopa group (0.50 ± 0.02 OD) also showed a significant decline in NRF2 expression compared to the MPTP group, & highly significant difference was observed when compared to AA-200 (Figure 8).

Effect of *A. agallocha* on brain LRRK2 levels

The MPTP group showed a significant reduction in LRRK2 expression (0.20 ± 0.01 OD) compared to the normal control group (0.88 ± 0.01 OD, #$p < 0.05$), suggesting neuronal damage and dysregulation of neuroinflammatory pathways. Treatment with *A. agallocha* resulted in a dose-dependent increase in LRRK2 levels. The AA-50 group showed a modest rise (0.35 ± 0.01 OD, *$p < 0.05$ vs MPTP), while AA-100 (0.52 ± 0.01 OD, **$p < 0.01$) and AA-200 (0.84 ± 0.01 OD, ***$p < 0.001$) significantly restored LRRK2 expression. The AA-200 group closely matched the NC group, indicating near-complete reversal of MPTP-induced suppression. The standard levodopa-treated group also restored LRRK2 levels (0.75 ± 0.01 OD), and no significant difference was observed between LD and AA-200 groups (ns), highlighting the comparable neuroprotective efficacy of *A. agallocha* at higher doses (Figure 8).

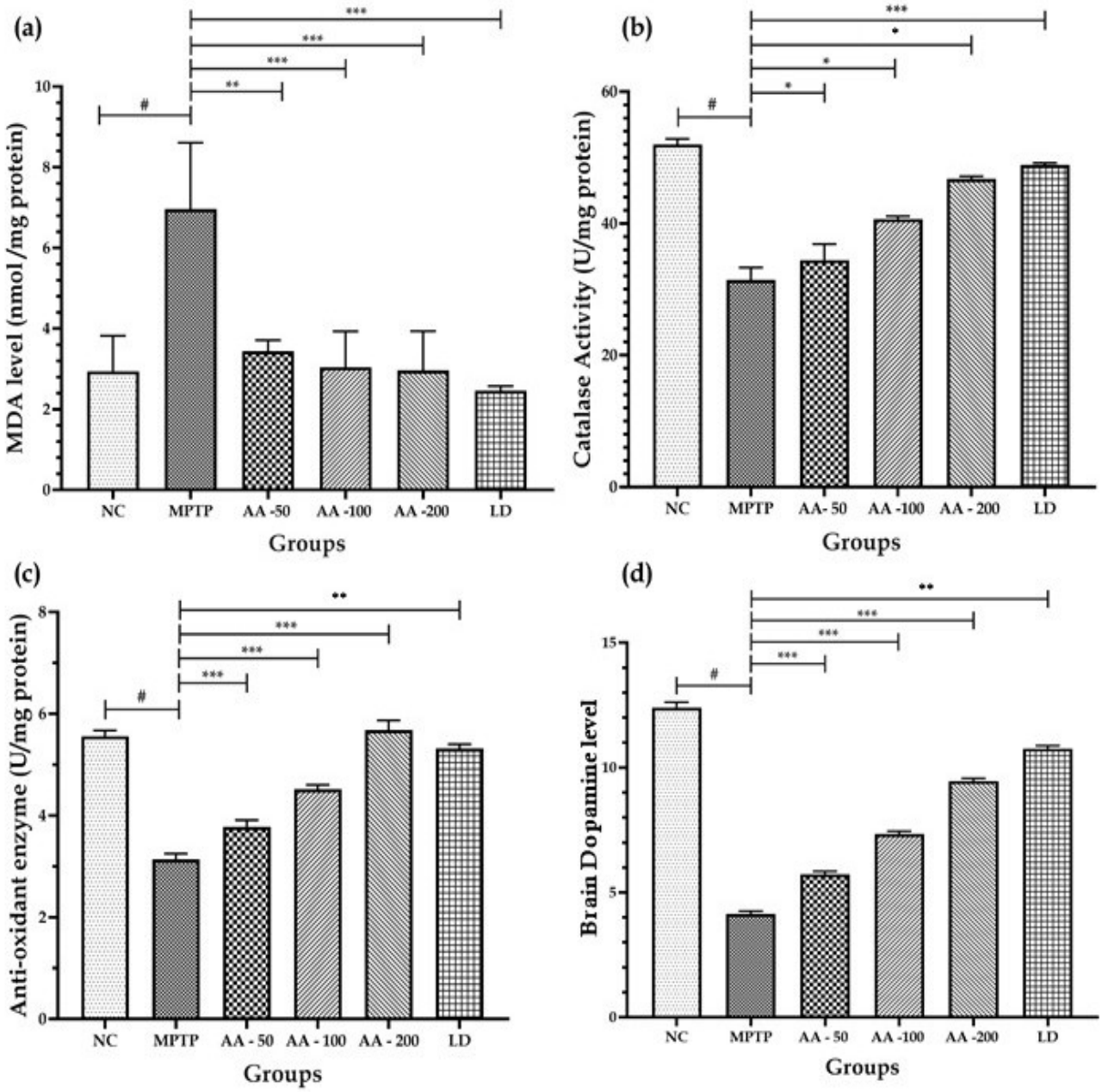

Figure 7: The antioxidant potential of *Aquilaria agallocha* depicted via (a) MDA, (b) Catalase, (c) Antioxidant enzyme (SOD), and (d) Neurotransmiter Dopamine levels in brain tissue on treatment with different groups. Data are expressed as mean ± SD (n=6) and analysed using one-way ANOVA followed by Tukey's multiple comparison test. #p<0.05 as compared to NC, *$p < 0.01$, **$p < 0.001$, ***$p < 0.0001$ vs MPTP group.

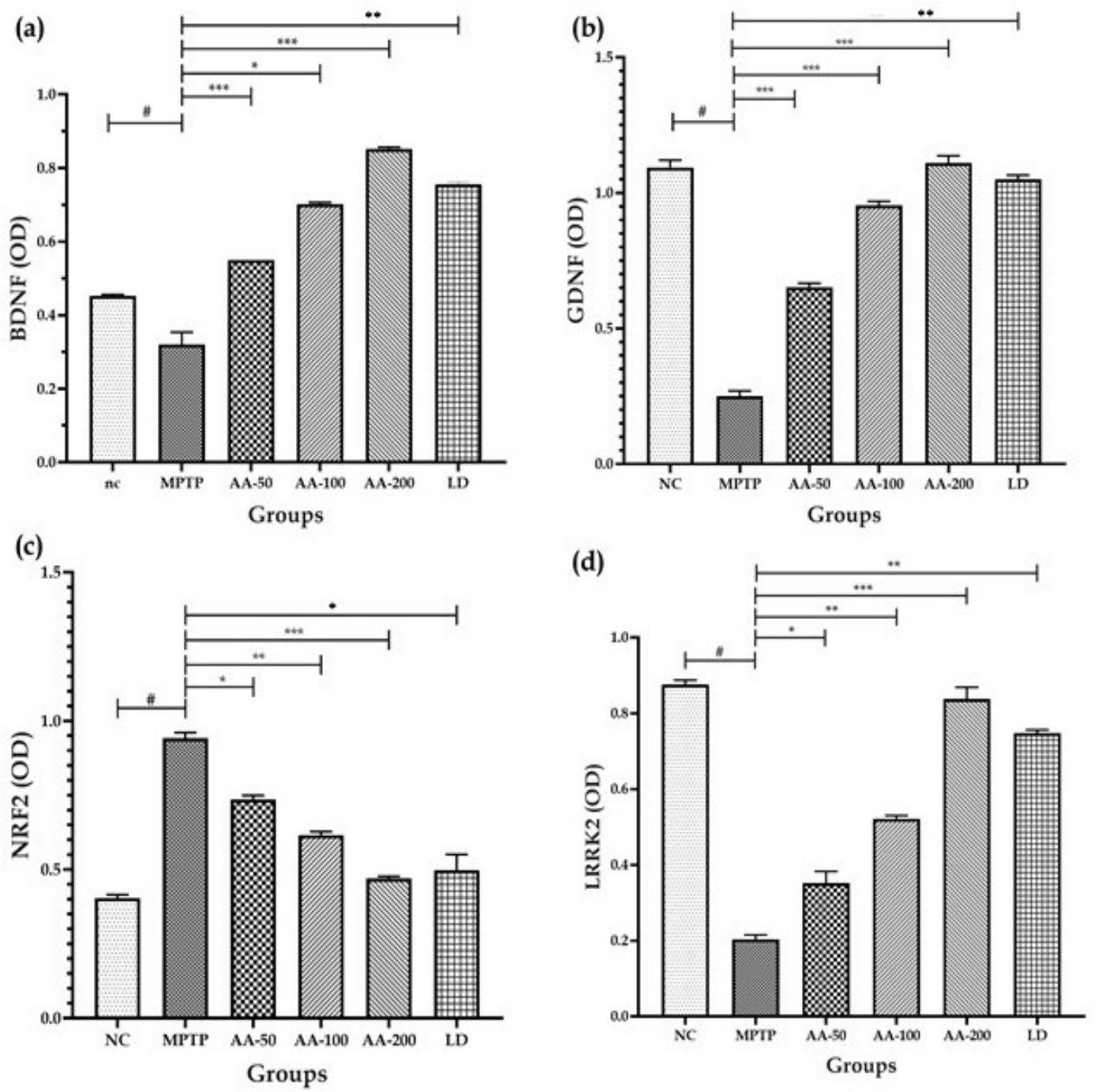

Figure 8: Effect of *Aquilaria agallocha* on expression of (a) BDNF, (b) GDNF, (c) NRF2, and (d) LRRK2 across treatment groups. Data are expressed as mean ± SD (n=6) and analysed using one-way ANOVA followed by Tukey's multiple comparison test. $^{\#}p<0.05$ as compared to NC, $^{*}p < 0.01$, $^{**}p < 0.001$, $^{***}p < 0.0001$ vs MPTP group, and ns: non-significant.

HISTOPATHOLOGY

The Normal Control (NC) group (Figure 9a) exhibited intact neuronal architecture with no signs of gliosis or neuronal degeneration, indicating normal histology. In contrast, the disease control (MPTP) group (Figure 9b) demonstrated extensive cellular damage, marked gliosis, neuronal shrinkage, necrosis, and the presence of Lewy body-like inclusions, suggesting severe dopaminergic neurodegeneration. Treatment with Levodopa (LD) (Figure 9c) and AA-50 (Figure 9d) resulted in partial neuroprotection, showing mild glial reactivity and focal individual neuronal degeneration. The AA-100 treated group (Figure 9e) exhibited notable protection with reduced glial activation and minimal neuronal damage, indicating better restoration of normal cytoarchitecture. Strikingly, the AA-200 group (Figure 9f) showed significant neuroprotection, as evidenced by near-normal glial morphology, reduced reactiveness, and preservation of neuronal structure, comparable to the normal group.

DISCUSSION

Parkinson's Disease (PD) is a progressive neurodegenerative disorder characterized by complex molecular pathogenesis involving apoptosis, inflammation, and mitochondrial dysfunction. In this experimental study, *Aquilaria agallocha* (AA) extract was investigated for its bioactive compounds and potential neuroprotective mechanisms using network pharmacology, enrichment analyses, molecular docking, and *in vivo* assays. Network pharmacology revealed that AA-derived bioactives target multiple molecular pathways implicated in PD. The constructed Protein–Protein Interaction (PPI) network consisted of 45 nodes and 700 edges, with an average node degree of 31.1, indicating a highly interconnected system. The high clustering coefficient (0.837) suggested the presence of tightly linked functional modules. The observed number of edges (700) was substantially higher than the expected number (247), with a PPI enrichment p-value < 1.0×10^{-16}, confirming the non-random and biologically relevant nature of the interactions (Figures 2 and 3) (Jeong *et al.*, 2018).

KEGG pathway enrichment analysis identified several PD-related pathways, including apoptosis (hsa04210), TNF signaling (hsa04668), PI3K–Akt signaling (hsa04151), and HIF-1 signaling (hsa04066), all of which are recognized for their roles in neuroinflammation, oxidative stress, and neuronal apoptosis. Additional enriched pathways included neurotrophin signaling (hsa04722) and mitophagy (hsa04137), both of which are critical for neuronal survival and mitochondrial homeostasis. Pathways associated with other neurodegenerative diseases, such as Alzheimer's disease (hsa05010) and amyotrophic lateral sclerosis (hsa05014), also emerged, suggesting that AA bioactives may target common pathological mechanisms in neurodegeneration (Table 1) (Khan *et al.*, 2024). Core network nodes such as MAPK3, MAPK1, and TP53 exhibited high connectivity (degree = 14; ASPL ≈ 2.0), reinforcing their central role in disease-related signaling. RELA, with the highest network diffusion efficiency (NDE = 12.15), emerged as a key regulatory hub (Khazdair *et al.*, 2021). Among the identified bioactives, 12-deoxyphorbol-13-(3E,5E-decadienoate) displayed the highest connectivity (degree = 40; ASPL = 1.59), whereas Clemiscosin D had a more peripheral role (ASPL = 2.67; BC = 0.02), indicating functional diversity in their potential mechanisms of action.

Gene Ontology (GO) enrichment analysis using the STRING database revealed significant enrichment in all three categories: Cellular Component (CC), Molecular Function (MF), and Biological Process (BP). In CC, the endomembrane system (GO:0012505) was most significantly enriched (FDR = 0.00032) with 27 associated genes. In MF, protein binding (GO:0005515) showed the highest significance (FDR = 1.17×10^{-14}) with 44 associated genes, while in BP, response to oxygen-containing compounds (GO:1901700) was the most enriched term (FDR = 6.40×10^{-31}), involving 38 genes. These findings support the involvement of AA targets in oxidative stress response, protein interactions, and intracellular localization processes relevant to PD pathogenesis (Figure 4) (Lakshmi *et al.*, 2023).

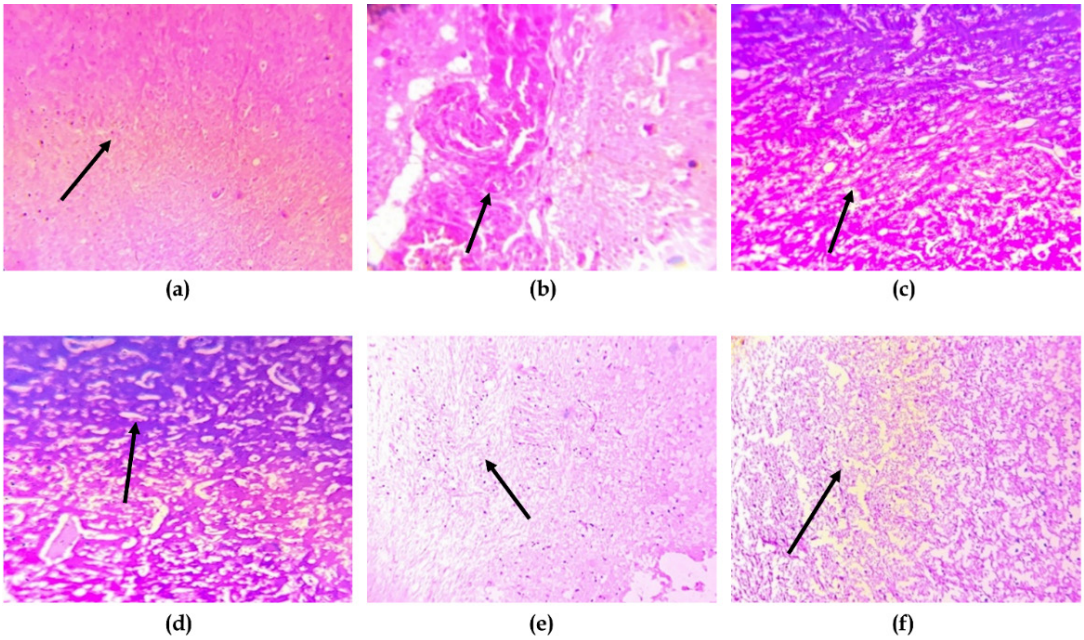

Figure 9: Histopathological examination of the striatum 40X in different groups along with *Aquilaria agallocha* treatments (a) NC-No Loss of glia reaction and loss of individual neuronal degeneration (black arrow), (b) DC-Cellular damage and gliosis, necrosis and shrinkage of dopaminergic neurons, Lewy body-like structures, (c) Std-mild glia reaction and individual neuronal degeneration (black arrow), (d) AA50- mild glia reaction and individual neuronal degeneration (black arrow), (e) AA100 - Good protection in glia cell with less reactiveness and neuronal degeneration (black arrow), (f) AA200 - Significant protection in glia cell with less reactiveness and neuronal degeneration (black arrow).

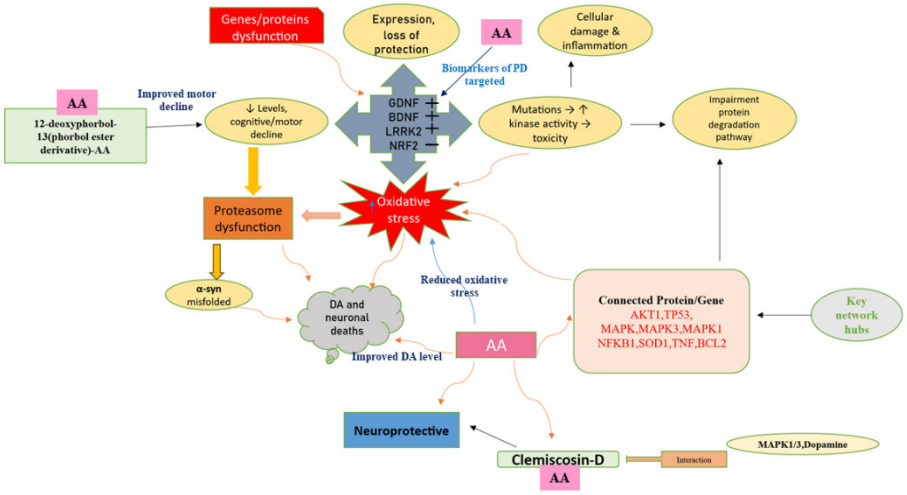

Figure 10: Mechanistic exploration of *Aquilaria agollacha* by *in vivo* and network pharmacology against Parkinson's disease. DA: Dopamine, AA: *Aquilaria agollacha.*

Molecular docking studies further supported the therapeutic potential of AA bioactives. 12-deoxyphorbol-13-(3E,5E-decadienoate) showed strong binding affinity with MAPK3 (–9.1 kcal/mol), forming hydrogen bonds with SER170, ASN171, and GLU50, and hydrophobic interactions with LEU124 and ILE48, suggesting a stable ligand–protein complex with potential regulatory effects on MAPK3 signaling (Zhang *et al.*, 2025). Clemiscosin D exhibited a comparable binding affinity for MAPK1 (–9.0 kcal/mol), engaging GLN103, ASP165, LYS52, and TYR34 via hydrogen bonds, along with hydrophobic contacts with VAL37 and ILE82. The Clemiscosin D–MAPK3 complex demonstrated the most favorable interaction profile, with short hydrogen bond distances (~3.91 Å), highlighting its potential as a dual MAPK1/MAPK3 modulator. Furthermore, Clemiscosin D showed notable binding with dopamine-associated targets (–8.9 kcal/mol), forming hydrogen bonds with ASN70 and PRO139, suggesting additional potential for supporting dopaminergic function impaired in PD (Sahu *et al.*, 2025; Saleem *et al.*, 2021).

In vivo studies in MPTP-induced PD models revealed that AA administration significantly attenuated oxidative stress. MPTP exposure elevated lipid peroxidation (MDA) and reduced catalase activity, consistent with oxidative injury. AA treatment reversed these effects in a dose-dependent manner, restoring catalase activity, reducing MDA levels, and enhancing the activity of antioxidant enzymes such as SOD. The highest dose of AA demonstrated comparable efficacy to levodopa, suggesting its potential as an adjunct therapy for oxidative stress in PD (Fathy *et al.*, 2021). Mechanistically, AA restored the expression of Brain-Derived Neurotrophic Factor (BDNF) and Glial cell line-Derived Neurotrophic Factor (GDNF), both of which are essential for synaptic plasticity, neuronal survival, and cognitive function. Restoration of LRRK2 expression, particularly at higher doses, further indicated a potential role in maintaining mitochondrial function and intracellular signaling. Although AA did not significantly augment Nrf2 expression beyond MPTP-induced levels, its strong antioxidant effects suggest action via parallel or downstream antioxidant pathways, potentially involving direct free radical scavenging (Wang *et al.*, 2010).

The Figure 10 observed oxidative stress plays a key role in Parkinson's disease by causing proteasome dysfunction, α-synuclein misfolding, and dopaminergic neuron loss. Compounds of AA and Clemscocin-D reduce oxidative damage, restore protective proteins (GDNF, BDNF, LRRK2, NRF2), and enhance dopamine signaling. Their combined action offers neuroprotection and may slow PD progression. Thus, modulation of oxidative stress and related pathways by AA and clemscocin-D may represent a promising therapeutic approach for neuroprotection and functional recovery in parkinson's disease.

CONCLUSION

The pathogenesis of Parkinson's Disease (PD) is closely associated with the interplay of genetic mutations, oxidative stress, proteasome dysfunction, and neuroinflammation. In this study, a network-based approach elucidated the molecular mechanisms involved in PD progression and highlighted the neuroprotective potential of phytoconstituents derived from *Aquilaria agallocha* (AA). Key neurodegenerative factors, including reduced expression of neuroprotective genes and proteins such as GDNF, BDNF, LRRK2, and NRF2, lead to impaired cellular homeostasis. Genetic mutations enhance kinase activity, resulting in cellular damage and chronic inflammation. This cascade increases oxidative stress, a central pathological hallmark of PD, and initiates downstream effects like proteasome dysfunction and α-synuclein

misfolding, ultimately causing dopaminergic neuronal death. Our study demonstrates that bioactive compounds such as 12-deoxyphorbol-13-acetate (a phorbol ester from AA), exert multi-targeted neuroprotective effects. These compounds inhibit oxidative stress, enhance proteasome function, modulate kinase activity, and restore protein degradation pathways. In silico docking and network pharmacology analyses revealed strong interactions between these phytochemicals and Key network hubs involved in signalling proteins, including MAPK1, MAPK3, AKT1, TP53, and NF-κB. Of particular interest is Clemiscosin-D, a compound showing potential regulatory influence on MAPK signalling and dopamine-related neuronal survival pathways. The synergistic action of AA constituents contributes significantly to neuroprotection by attenuating dopaminergic degeneration and restoring cellular balance. The modulation of oxidative stress and proteostasis by phytochemicals from *Aquilaria agallocha* offers promising therapeutic potential in managing PD.

ACKNOWLEDGEMENT

Authors are thankful to Ramanbhai Patel College of Pharmacy, Charotar University of Science and Technology for the necessary support during the study.

ABBREVIATIONS

PD: Parkinson's Disease; **GDNF:** Glial Cell Line–Derived Neurotrophic Factor; **BDNF:** Brain-Derived Neurotrophic Factor; **LRRK2:** Leucine-Rich Repeat Kinase; **NRF2:** Nuclear Factor Erythroid 2–Related Factor 2; **TRABS:** Transcriptional Regulatory Binding Sites; **SOD:** Superoxide Dismutase; **ELISA:** Enzyme-Linked Immunosorbent Assay; **PI3K-Akt:** Phosphoinositide 3-Kinase – Protein Kinase B; **NF-κB:** Nuclear Factor Kappa-Light-Chain-Enhancer of Activated B Cells; **ROS:** Reactive Oxygen Species; **NMDA:** N-Methyl-D-Aspartate; **µM (uM):** Micromolar (10^{-6} Molar, Concentration Unit); **MPTP:** 1-Methyl-4-Phenyl-1,2,3,6-Tetrahydropyridine (Neurotoxin Used to Induce PD Models); **NBT:** Nitro Blue Tetrazolium; **TP53:** Tumor Protein 53; **RELA:** p65 Subunit of NF-κB Transcription Factor; **NFKB1:** p50 Subunit of NF-κB Transcription Factor; **TNF:** Tumor Necrosis Factor; **OD:** Optical Density.

CONFLICT OF INTEREST

The authors declare that there is no conflict of interest.

ETHICAL APPROVAL

The study was ethically approved in IAEC-CCSEA (Protocol no. - PIPR985/2023/01/02).

REFERENCES

Abolarin, P. O., Amin, A., Nafiu, A. B., Ogundele, O. M., & Owoyele, B. V. (2024). Optimization of Parkinson's disease therapy with plant extracts and nutrition's evolving roles. In IBRO Neuroscience Reports. Elsevier, 17, 1–12. https://doi.org/10.1016/j.ibneur.2024.05.011

Abushouk, A. I., Negida, A., Ahmed, H., & Abdel-Daim, M. M. (2017). Neuroprotective mechanisms of plant extracts against MPTP induced neurotoxicity: Future applications in Parkinson's disease. In Biomedicine and Pharmacotherapy. Elsevier Masson SAS, 85, 635–645. https://doi.org/10.1016/j.biopha.2016.11.074

Alam, J., Mujahid, M., Badr, B., Rahman, M., Akhtar, J., Khalid, M., Jahan, Y., Basit, A., Khan, A., Shawwal, M., & Iqbal, S. (2015). An insight of pharmacognostic study and phytopharmacology of *Aquilaria agallocha*. Journal of Applied Pharmaceutical Science, 173–181. https://doi.org/10.7324/JAPS.2015.50827

Ashok Giri, M., Bhalke, R. D., Prakash, K. V., & Kasture, S. B. (2020). Antiparkinsonian and Antioxidant Effects of hydroalcoholic extract of *Camellia sinensis, Asparagus racemosus, Mucuna pruriens* and their Combination. International Journal of Pharmaceutical Investigation, 10(4), 569–574. https://doi.org/10.5530/ijpi.2020.4.99

Bagewadi, H. G., R., V., & Zahid, S. H. (2018). Rotarod test and Catalepsy Bar Test: Behavioral testing and neuromodulation of *Aloe vera* in MPTP induced Parkinson's disease animal model. International Journal of Basic and Clinical Pharmacology, 7(3), 494. https://doi.org/10.18203/2319-2003.ijbcp20180663

Chen, J., Shi, X., Chen, Y., Liang, H., Cheng, C., & He, Q. (2018). Neuroprotective effects of chloroform and aqueous fractions of noni juice against t-butyl hydroperoxide-induced oxidative damage in SH-SY5Y cells. Food and Nutrition Research, 62. https://doi.org/10.29219/fnr.v62.1605

Corona, J. C. (2018). Natural compounds for the management of Parkinson's disease and attention-deficit/hyperactivity disorder. In BioMed Research International. Hindawi Publishing Limited, 2018, Article 4067597. https://doi.org/10.1155/2018/4067597

Dash, M., Kumar Patra, J. *et al.* (2008). Phytochemical and antimicrobial screening of extracts of *Aquilaria agallocha* Roxb. Ethnobotany of Dioscorea species View project Ethnobotanical Documentatiobn View project Phytochemical and antimicrobial screening of extracts of *Aquilaria agallocha* Roxb. African Journal of Biotechnology, 7(20), 3531–3534. https://doi.org/10.5897/AJB08.623

Delenclos, M., Burgess, J. D., Lamprokostopoulou, A., Outeiro, T. F., Vekrellis, K., & McLean, P. J. (2019). Cellular models of alpha-synuclein toxicity and aggregation. In Journal of Neurochemistry. Blackwell Publishing Limited, 150(5), 566–576. https://doi.org/10.1111/jnc.14806

Duyu, T., Khanal, P., Ashrafali Khatib, N., & Mahadevagouda Patil, B. (2020). *Mimosa pudica* modulates neuroactive ligand-receptor interaction in Parkinson's disease. Indian Journal of Pharmaceutical Education and Research, 54(3), 732–739. https://doi.org/10.5530/ijper.54.3.124

Fathy, S. M., El-Dash, H. A., & Said, N. I. (2021). Neuroprotective effects of pomegranate (*Punica granatum* L.) juice and seed extract in paraquat-induced mouse model of Parkinson's disease. BMC Complementary Medicine and Therapies, 21(1), Article 130. https://doi.org/10.1186/s12906-021-03298-y

Gopi, C., Sastry, V. G., & Dhanaraju, M. D. (2019). Effect of novel phenothiazine derivatives on brain dopamine in Wistar rats. Beni-Suef University Journal of Basic and Applied Sciences, 8(1). https://doi.org/10.1186/s43088-019-0007-y

Gopinath, K., & Sudhandiran, G. (2015). Protective effect of naringin on 3-nitropropionic acid-induced neurodegeneration through the modulation of matrix metalloproteinases and glial fibrillary acidic protein. Canadian Journal of Physiology and Pharmacology, 94(1), 65–71. https://doi.org/10.1139/cjpp-2015-0035

Hashim, Y. Z. H.-Y., Kerr, P. G., Abbas, P., & Mohd Salleh, H. (2016). *Aquilaria* spp. (agarwood) as source of health beneficial compounds: A review of traditional use, phytochemistry and pharmacology. In Journal of Ethnopharmacology. Elsevier Ireland Limited, 189, 331–360. https://doi.org/10.1016/j.jep.2016.06.055

Jeong, J. S., Piao, Y., Kang, S., Son, M., Kang, Y. C., Du, X. F., Ryu, J., Cho, Y. W., Jiang, H.-H., Oh, M. S., Hong, S.-P., Oh, Y. J., & Pak, Y. K. (2018). Triple herbal extract DA-9805 exerts a neuroprotective effect via amelioration of mitochondrial damage in experimental models of Parkinson's disease. Scientific Reports, 8(1), Article 15953. https://doi.org/10.1038/s41598-018-34240-x

Khan, A., Ullah, F., Alkreathy, H. M., Ahmed, M., & Khan, R. A. (2024). Phytochemical screening, antioxidant and anti-Parkinson activities of *Berula erecta*: A novel medicinal plant. PLOS One, 19(11), Article e0305751. https://doi.org/10.1371/journal.pone.0305751

Khazdair, M. R., Kianmehr, M., & Anaeigoudari, A. (2021). Effects of medicinal plants and flavonoids on Parkinson's disease: A review on basic and clinical evidences. In Advanced Pharmaceutical Bulletin. Tabriz University of Medical Sciences, 11(2), 224–232. https://doi.org/10.34172/apb.2021.026

Kumaree, K. K., Brimson, J. M., Verma, K., Chuchawankul, S., Tencomnao, T., & Prasansuklab, A. (2025). Agarwood leaf ethanol extract provides neuroprotective properties and promotes cholinergic differentiation of HT22 hippocampal neurons. Scientific Reports, 15(1), Article 10230. https://doi.org/10.1038/s41598-025-93462-y

Lakshmi, Y. S., Prasanth, D. S. N. B. K., Kumar, K. T. S., Ahmad, S. F., Ramanjaneyulu, S., Rahul, N., & Pasala, P. K. (2023). Unravelling the molecular mechanisms of a quercetin nanocrystal for treating potential Parkinson's disease in a rotenone model: Supporting evidence of network pharmacology and in silico data analysis. Biomedicines, 11(10), Article 2756. https://doi.org/10.3390/biomedicines11102756

Leão, A. H. F. F., Meurer, Y. S. R., da Silva, A. F., Medeiros, A. M., Campêlo, C. L. C., Abílio, V. C., Engelberth, R. C. G. K., Cavalcante, J. S., Izídio, G. S., Ribeiro, A. M., & Silva, R. H. (2017). Spontaneously hypertensive rats (SHR) are resistant to a reserpine-induced progressive model of Parkinson's disease: Differences in motor behavior, tyrosine hydroxylase and α-synuclein expression. Frontiers in Aging Neuroscience, 9, Article 78. https://doi.org/10.3389/fnagi.2017.00078

Lee, C. H., Lee, T. H., Ong, P. Y., Wong, S. L., Hamdan, N., Elgharbawy, A. A. M., & Azmi, N. A. (2021). Integrated ultrasound-mechanical stirrer technique for extraction of total alkaloid content from *Annona muricata*. Process Biochemistry, 109, 104–116. https://doi.org/10.1016/j.procbio.2021.07.006

Li, J., Zhang, M., Yu, C.-Q., Xue, M., & Hu, P.-P. (2025). Early diagnosis of Parkinson's disease: Biomarker study. In Frontiers in Aging Neuroscience, 17. Frontiers Media SA, Article 1495769. https://doi.org/10.3389/fnagi.2025.1495769

Miniyar, P. B., Chitre, T. S., Deuskar, H. J., Karve, S. S., & Jain, K. (2008). Antioxidant activity of ethyl acetate extract of *Aquilaria agallocha* on nitrite-induced methaemoglobin formation. International Journal of Green Pharmacy, 2(2), 116. https://doi.org/10.4103/0973-8258.41185

Oraon, R., Ansari, M., Shamim, A., Bagga, P., Ahsan, F., Alam, M., Parveen, S., *et al.* (2019). World Journal of Pharmaceutical Sciences Pharmacological potentials of *Aquilaria agallocha* & *Borago officinalis*: A pragmatic review. World J. PharmSci, 7(4), 43–55. http://www.wjpsonline.org/

Rahman, H., Vakati, K. *et al.* (2012). *In vivo* and *in vitro* anti-inflammatory activity of *Aquilaria agallocha* oil Phytochemical and Pharmacological evaluation of *Citrus macroptera* Var. *Annamensis* and *Oryza sativa* Var. Joha Rice. Medicinal Plants of Assam View project Formulation and evaluation of microspheres for treatment of ulcerative colitis using natural gums View project *in vivo* and *in vitro* anti-inflammatory Activity of *Aquilaria agallocha* Oil. In International Journal of Basic Medical Sciences and Pharmacy (IJBMSP) (Vol., Issue https://www.researchgate.net/publication/288256061, 2.

Rao, S. P., Sharma, N., & Kalivendi, S. V. (2020). Embelin averts MPTP-induced dysfunction in mitochondrial bioenergetics and biogenesis via activation of SIRT1. Biochimica et Biophysica Acta. Bioenergetics, 1861(3), Article 148157. https://doi.org/10.1016/j.bbabio.2020.148157

Ravi, S. K., Narasingappa, R. B., Joshi, C. G., Girish, T. K., & Vincent, B. (2018). Neuroprotective effects of Cassia Tora against paraquatinduced neurodegeneration: Relevance for Parkinson's disease. Natural Product Research, 32(12), 1476–1480. https://doi.org/10.1080/14786419.2017.1353504

Sahu, M. K., Shrivastava, S., & Thakur, A. (2025). Explores the network pharmacology and molecular docking-based prediction of the molecular target and signaling pathways of piperine in the treatment of Parkinson's disease. Research Square. https://doi.org/10.21203/rs.3.rs-6097620/v1

Saleem, U., Bibi, S., Shah, M. A., Ahmad, B., Saleem, A., Chauhdary, Z., Anwar, F., Javaid, N., Hira, S., Akhtar, M. F., Shah, G. M., Khan, M. S., Muhammad, H., Qasim, M., Alqarni, M., Algarni, M. A., Blundell, R., Vargas-De-La-Cruz, C., Herrera-Calderon, O., & Alhasani, R. H. (2021). Anti-Parkinson's evaluation of *Brassica juncea* leaf extract and underlying mechanism of its phytochemicals. Frontiers in Bioscience, 26(11), 1031–1051. https://doi.org/10.52586/5007

Sikdar, D., Saha, S., Barua, B. *et al.* (2017). Phytochemical screening, phenolic content and antioxidant activity of wild date palm (*Phoenix sylvestris* Roxb.) fruit extracted with different solvents Pharmacological effects of indigenous fruits of Bangladesh View project Phytochemical screening, phenolic content and antioxidant activity of wild date palm (*Phoenix sylvestris* Roxb.) fruit extracted with different solvents. In International Food Research Journal, 24(6).

Subramanian, G., Fanai, H. L., Chand, J., Ahmad, S. F., Attia, S. M., & Emran, T. B. (2024). System biology-based assessment of the molecular mechanism of IMPHY000797 in Parkinson's disease: A network pharmacology and *in silico* evaluation. In Scientific Reports, 14(1), Article 23414. https://doi.org/10.1038/s41598-024-75603-x

Tanaka, K., Galduróz, R. F., Gobbi, L. T., & Galduróz, J. C. (2013). *Ginkgo biloba* extract in an animal model of Parkinson's disease: A systematic review. In Current Neuropharmacology, 11(4)(4), 430–435. https://doi.org/10.2174/1570159X11311040006

Tang, Y., & Le, W. (2016). Differential roles of M1 and M2 microglia in neurodegenerative diseases. In Molecular Neurobiology. Humana Press, Incorporated, 53(2), 1181–1194. https://doi.org/10.1007/s12035-014-9070-5

Wang, S., Yu, Z., Wang, C., Wu, C., Guo, P., & Wei, J. (2018). Chemical constituents and pharmacological activity of agarwood and Aquilaria plants. In Molecules. MDPI, 23(2), Article 342. https://doi.org/10.3390/molecules23020342

Wang, Y.-H., Samoylenko, V., Tekwani, B. L., Khan, I. A., Miller, L. S., Chaurasiya, N. D., Rahman, M. M., Tripathi, L. M., Khan, S. I., Joshi, V. C., Wigger, F. T., & Muhammad, I. (2010). Composition, standardization and chemical profiling of Banisteriopsis caapi, a plant for the treatment of neurodegenerative disorders relevant to Parkinson's disease. Journal of Ethnopharmacology, 128(3), 662–671. https://doi.org/10.1016/j.jep.2010.02.013

Xie, Y., Song, L., Li, C., Yang, Y., Zhang, S., Xu, H., Wang, Z., Han, Z., & Yang, L. (2021). Eudesmane-type and agarospirane-type sesquiterpenes from agarwood of *Aquilaria agallocha*. Phytochemistry, 192, Article 112920. https://doi.org/10.1016/j.phytochem.2021.112920

Zheng, H., Gao, J., Man, S., Zhang, J., Jin, Z., & Gao, W. (2019). The protective effects of Aquilariae Lignum Resinatum extract on 5-Fuorouracil-induced intestinal mucositis in mice. Phytomedicine, 54, 308–317. https://doi.org/10.1016/j.phymed.2018.07.006

Cite this article: Shukla P, Solanki N, Dwivedi PSR. *Aquilaria agallocha* Mitigates MPTP Induced Parkinson's Disease by Targeting the BDNF/GDNF and NRF2 Pathways: A Network Pharmacology and an *in vivo* Study. Pharmacog Res. 2026;18(2):460-75